Proceedings of the ASME 2011
30th International Conference on Ocean, Offshore and Arctic Engineering
OMAE2011
June 19-24, 2011, Rotterdam, The Netherlands

OMAE2011-49593

WAVE PATTERNS, WAVE INDUCED FORCES AND MOMENTS FOR A GRAVITY BASED STRUCTURE PREDICTED USING CFD

Worakanok Thanyamanta
Oceanic Consulting Corporation
St. John's, NL
Canada

Paul Herrington
Oceanic Consulting Corporation
St. John's, NL
Canada

David Molyneux
Oceanic Consulting Corporation
St. John's, NL
Canada

ABSTRACT

Gravity Based Structures (GBSs) are commonly used in the offshore oil and gas industry for storage during the production of hydrocarbons. The GBS sits on the sea bed, but it is subjected to forces and moments caused by waves. Obtaining accurate predictions of the magnitude of wave induced forces and bending moments is essential input to the structural design. Other key operational factors are the wave field in the vicinity of the structure and the amount of green water that will come onto the deck of the GBS.

Scale model experiments can be used to obtain these predictions but this is an expensive option, especially in the early stages of a design, when many different concepts may be considered. An alternative method is to use Computational Fluid Dynamics (CFD). One CFD approach that is particularly suited to the challenges of predicting the required performance parameters for a GBS is the Volume of Fluid method, which is available in the commercial code *Flow-3D*.

This paper presents the numerical simulation of the wave field around a surface piercing cylinder using the Volume of Fluid approach and compares it to published results. It also presents the simulations of the forces, moments and wave field around a proposed Gravity Based Structure, for which model data was available. The results show that predictions made using the Volume of Fluid method agree well with the observed wave patterns close to the structure in both cases, and that the method also gives good predictions of the observed forces and bending moments acting on the GBS.

INTRODUCTION

In the offshore oil and gas industry Gravity Based Structures (GBSs) are commonly used for storage during the production of hydrocarbons. The performance of these structures in ocean waves is influenced by the magnitude of wave-induced forces and bending moments as well as amount of green water coming onto the deck. Designing a GBS requires accurate evaluation of these parameters. In the early stages of the design process, CFD can be used to quickly evaluate different design concepts, provided that the results are accurate. In order to assess the accuracy of the methods, they should be compared with the equivalent measurements from model experiments or full scale.

This paper presents the results of numerical simulations using a commercial RANS CFD code. *Flow-3D* is based on the Volume of Fluid (VOF) method that is particularly suited for predicting performance parameters of surface piercing structures. The simulations were carried out for two cases for which the equivalent data were available from model experiments.

The first case is the one used by the International Towing Tank Conference Offshore Committee as benchmark data for validating CFD codes. These data were for the wave patterns around a surfacing piercing cylinder. The second case was for a proposed concrete gravity caisson (CGC), which was to be a part of an LNG terminal. In these experiments, the performance of a proposed CGC was observed under various wave and current conditions. Global hydrodynamic forces, local impact pressures, and wave run-ups on the CGC were measured.

CFD SIMULATION

The CFD code used in this study applies the finite-volume method based on the full Navier Stokes and continuity equations. A three-dimensional, transient flow model is used which is capable of capturing nonlinearities within the wave patterns induced by the existence of the GBS. Moreover, the

surface capturing technique used in the code also allows for relatively steep and breaking waves [1].

In order to simulate the free surface of the fluid, *Flow-3D* employs the VOF method. The interface between gas and liquid represents the liquid free surface. Motion of the gas adjacent to the gas-liquid interface is neglected. The free surface is included in the model as an external boundary of a "one-fluid" problem (liquid phase in this case) with uniform pressure and temperature across the interface. Liquid volume fraction in each cell is then used to describe the motion of the free surface.

Using a finite difference approach, the computational domain is discretized into a finite number of rectangular cells forming a structured-type computational mesh block. Non-uniform grid spacing is also allowed in *Flow-3D*. Each cell is associated with the governing equations necessary for solving fluid motion as well as local average dependent variables.

In most cases a semi-implicit scheme is used to solve the governing equations. Using this approach, an explicit finite difference scheme is used for most terms but pressures and velocities are coupled implicitly. The types and number of equations required to solve each hydrodynamic problem are different. For wave problems, in addition to the equations for fluid flow, equations describing the waves are also needed at the Wave Boundary (see Flow-3D manual [2] for more detail).

The Wave Boundary allows simple generation of waves with various heights and frequencies. Linear or Stokes waves can be selected. The generation of irregular waves is also possible by using superposition of regular wave components. To minimize reflection of waves exiting the computational domain in wave propagation problems, the Sommerfeld radiation boundary condition is used at the end of the computing region (referred to as Outflow Boundary [2]). Even though the Outflow Boundary is used, the computational mesh should be designed in such a way that the first wave reaches the boundary at or after the end of simulation time.

In *Flow-3D*, solid surfaces within the computational domain are defined by a discretized mesh block used for fluid flow calculations. For each cell, the fractional surface area and fractional volume available for fluid flow are calculated using the FAVOR^{TM} (Fractional Area/Volume Obstacle Representation) method [2]. Incorporating all the solid components that are impermeable to the flow, the region open for fluid flow in the mesh block can then be determined and used for simulations. As solid surface representation is affected by the discretization of the computational domain, a sufficiently fine mesh is necessary. The required grid size can be determined using a grid sensitivity analysis. Forces and moments on solid structures can be computed at different times and locations in *Flow-3D*.

CFD CODE VALIDATION

In this study, the CFD code was validated by comparing simulation results with published results and available experimental data. The focus was the interaction between regular waves (of constant amplitude and frequency) and surface piercing structures. The parameters of interest included free surface elevations around the structure and wave induced forces and moments, depending on availability of experiment data.

ITTC Benchmark Data

Trulsen and Teigen [3] presented some experimental results which were used as a part of this study. The physical model tests were part of a study of the wave field around a surface piercing cylinder. In full scale, the cylinder had a diameter of 16 m diameter and extended 24 meters below the mean water level. The model tests were performed at a scale of 1:48.9. Two cases of regular waves were available. One case was for a wave height of 4.22 m with 9 second period. The second was for a wave height of 7.9 m with 9 second periods. Free surface elevations around the cylindrical structure were measured using wave probes at locations as shown in Figure 1. Forces and bending moments on the structure were not measured.

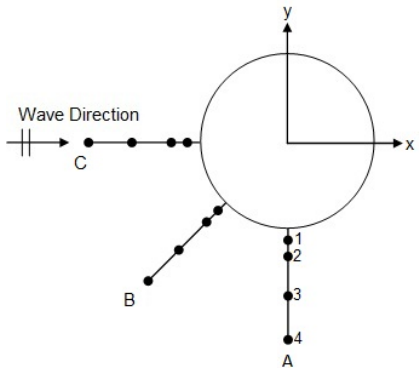

Figure 1. WAVE PROBE LOCATIONS [3]

A mesh block similar to the one used by Trulsen and Teigen [3] was created on model scale of 1:48.9. In full scale, a mesh block of length 921.6, half-width 230.4, and depth 200 m was used. Cartesian coordinates were used with the origin located at the centre of the cylinder and the bottom of the tank. Waves were generated at the Wave Boundary (–x boundary) and travelled along the x-direction to exit the computational domain at the +x boundary which was assigned an Outflow Boundary condition. Only half of the cylinder was simulated with a symmetry plane (Symmetry Boundary condition) applied at y = 0. At the –y boundary (right hand side of the y-axis when looking in the +x direction) and +z (upward direction) boundary were also applied Symmetry Boundary conditions. The bottom of the tank (z = 0) was assigned a Wall Boundary condition. In full scale, the mesh was discretized to have $\Delta x = \Delta y = 1.8$ m similar to that used in Trulsen and Teigen [3]. In the vertical direction, $\Delta z = 0.73$ m was chosen based on the horizontal discretization in order to avoid adverse cell aspect ratios and provide sufficient vertical discretization. With

the total active cells of 8.69 million, the required computational time varied between 0.5 and 1 day for the 4.22 m and 7.9 m waves, respectively using a 4-processor computer and double precision. Approximately 8 wave periods were simulated. Semi-implicit solving scheme was used with implicit pressure solving scheme. First-order momentum advection was selected and Split Lagrangian method was used to resolve fluid surface elevations.

Results from *Flow-3D* simulations and measurements from the physical model tests were compared. Figure 2 shows a 3D captured image of the simulated wave tank with the cylindrical structure. Figure 3 shows 2D images of velocity vectors and wave run-ups as the 4.22 m wave passed the cylindrical structure.

It can be seen from Figures 4 to 6 that the CFD code used in this study provided results that are consistent with the experimental data. Figure 5 shows its ability to capture non-linear effects caused by the cylinder's obstruction to the flow. In Figure 6, the code predicted wave diffraction around the cylinder very well. The predicted average maximum crest heights (relative to the undisturbed water level) at different locations were close to the measured data with similar trends of height variation around the structure. The results for locations near (e.g. probe A1) and further away (probe A4) from the cylinder wall matched equally well with the experimental data. Moreover, predicted values from the 4.22 m and 7.9 m cases showed the sufficiency of the vertical mesh resolution. Using the same vertical discretization, the 7.9 m wave had a finer vertical discretization than the 4.22 m wave (approximately 10.8 points compared to 5.7 points over a wave height). Regardless of that, the predicted surface elevations agreed well with experimental data for both wave heights. Moreover, an inviscid simulation of the 4.22 m wave showed that shear force on the cylinder was negligible and pressure force dominated in this problem.

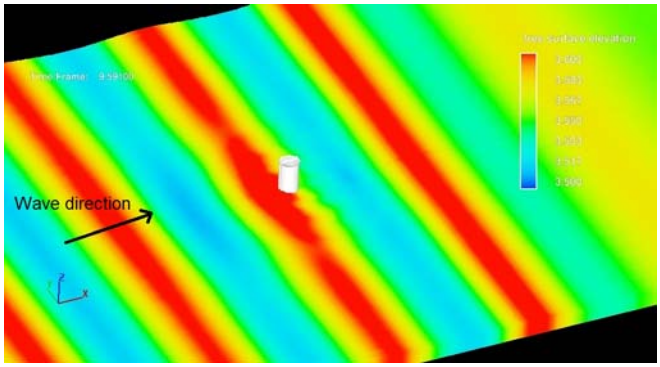

Figure 2. 3D IMAGE OF THE ITTC BENCHMARK WAVE TANK SIMULATION OF 4.22 M WAVE (MODEL SCALE)

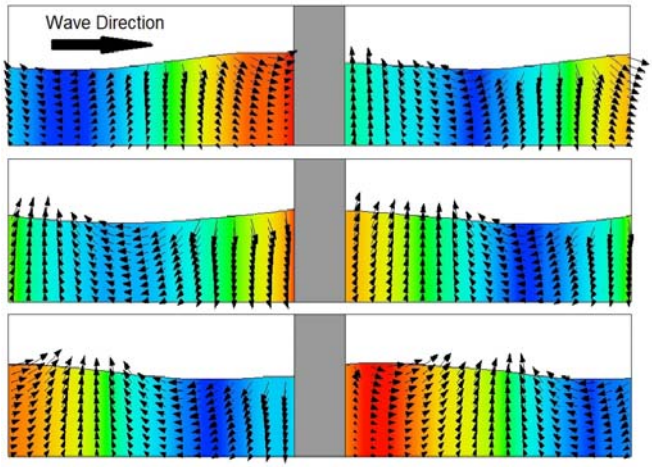

Figure 3. 2D IMAGES OF THE ITTC BENCHMARK WAVE TANK SIMULATION OF 4.22 M 9 SEC WAVE SHOWING RUN-UPS OF THE WAVE ON THE CYLINDRICAL STRUCTURE AT 9.59 SEC (TOP), 9.79 SEC (MIDDLE), AND 10 SEC (BOTTOM)

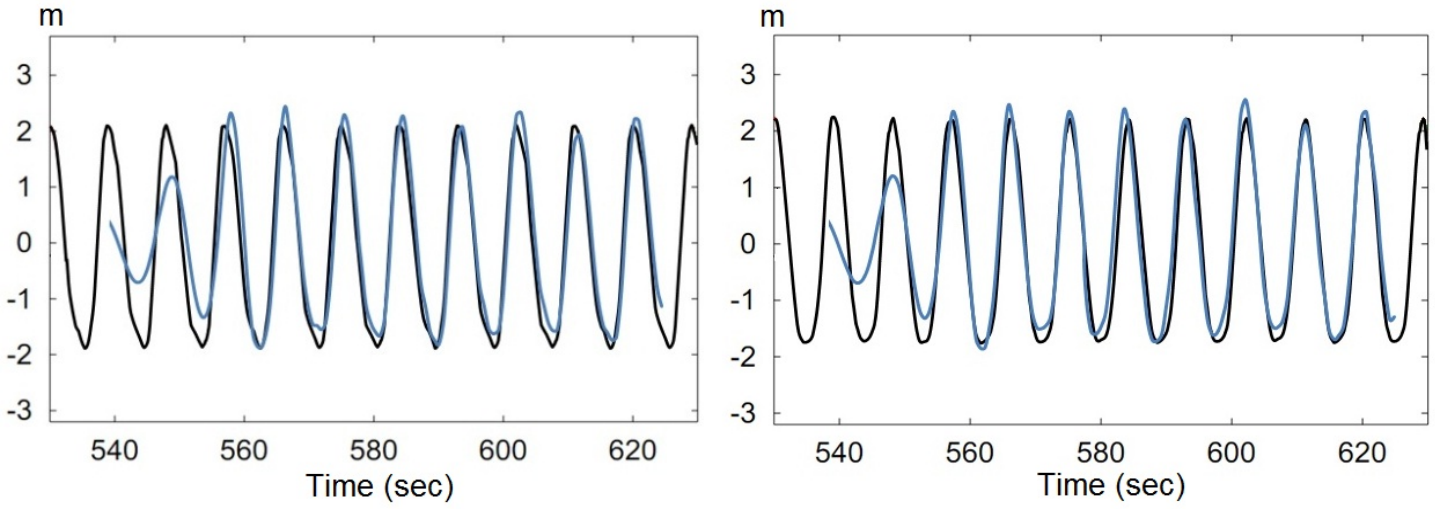

Figure 4. VARIATION OF FREE SURFACE ELEVATION FROM CALM WATER LEVEL FOR 4.22 M 9 SEC WAVE AT PROBE A3 (LEFT) AND A4 (RIGHT); COMPARISONS BETWEEN RESULTS FROM FLOW-3D SIMULATION (BLUE) AND ITTC BENCHMARK (BLACK) AS PUBLISHED IN TRULSEN AND TEIGEN [3]

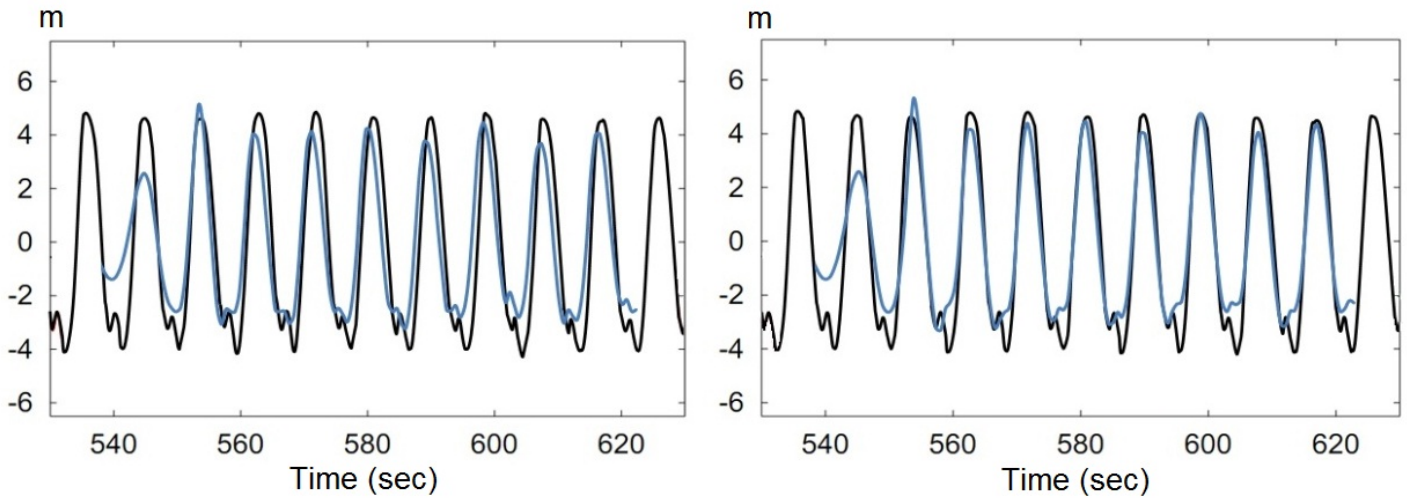

Figure 5. VARIATION OF FREE SURFACE ELEVATION FROM CALM WATER LEVEL FOR 7.9 M 9 SEC WAVE AT PROBE A3 (LEFT) AND A4 (RIGHT); COMPARISONS BETWEEN RESULTS FROM FLOW-3D SIMULATION (BLUE) AND ITTC BENCHMARK (BLACK) AS PUBLISHED IN TRULSEN AND TEIGEN [3]

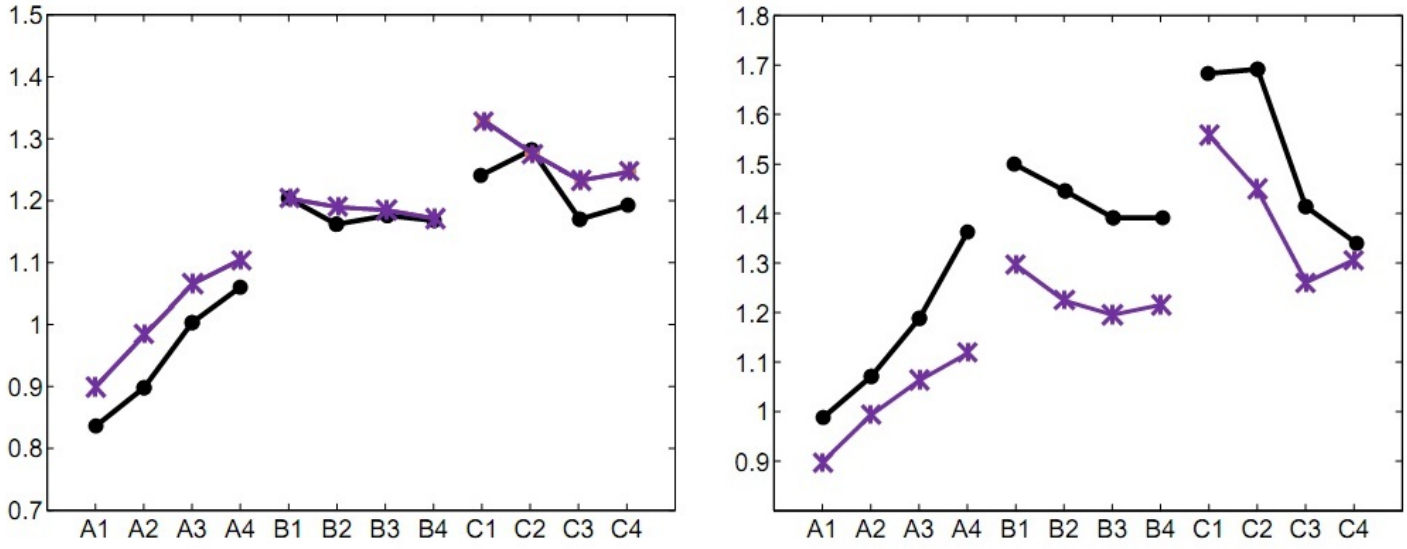

Figure 6. NORMALIZED AVERAGE MAXIMUM CREST HEIGHTS FOR 4.22 M 9 SEC WAVE (LEFT) AND 7.9 M 9 SEC WAVE (RIGHT); COMPARISONS BETWEEN RESULTS FROM FLOW-3D SIMULATION (PURPLE) AND ITTC BENCHMARK DATA (BLACK) AS PUBLISHED IN TRULSEN AND TEIGEN [3]

LNG Terminal Performance Evaluation

Oceanic Consulting Corporation also had measurements from experiments for a GBS with the geometry shown in Figure 7. Forces, bending moments and wave run-ups were measured for various wave heights and periods in order to study the loads and wave fields around the structure. Locations of wave measuring probes used in the experiments are shown in Figure 8. The lower probes were installed on the tank bottom close to the base of the structure and the upper probes were installed on the surface of the GBS base. There were three regular wave cases in the experimental study. Two cases of regular waves with different wave periods of 6.9 and 8.4 sec but with the same wave height of 5.5 m were used in this study. As these were shallow water cases (mean water level was 23.55 m), the third case with wave height of 10.31 m at the centre of the structure was unable to be studied numerically as the waves became unstable.

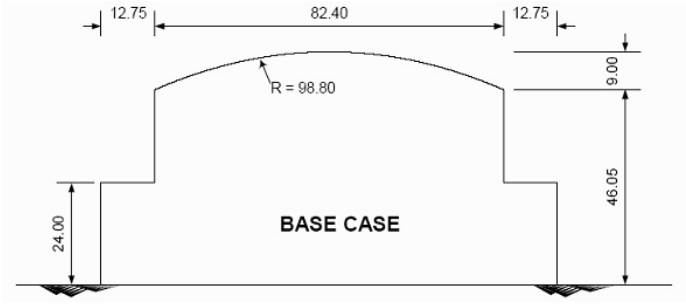

Figure 7. PROPOSED GBS STRUCTURE (FULL SCALE)

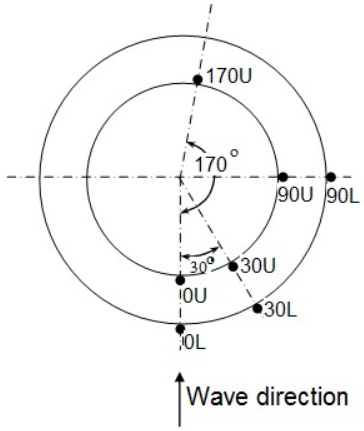

Figure 8. WAVE PROBE LOCATIONS AROUND THE GBS STRUCTURE

Grid Sensitivity Analysis

In Flow-3D, solid surface representation is affected by the resolution of the mesh block used. Therefore, even though the mesh block resolution is able to provide uniform wave pattern traveling along the length of the domain, sensitivity of simulation results to mesh resolution needs to be investigated in order to find the mesh that provides converged solutions. According to the ITTC Recommended Procedures and Guidelines [4], three meshes were used to simulate the aforementioned regular wave cases (5.5 m 6.9 sec and 5.5 m 8.4 sec waves). Mesh refinement ratio of $2^{1/2}$ was recommended by the ITTC [4]. Three grid refinements were used and the simulations were performed on model scale (1:40). The finest mesh had cell sizes as presented in Figure 9. The cell size was uniform close to the structure and gradually increased in x- and y-direction until maximum near the tank walls. A refinement ratio of $2^{1/2}$ was then used to increase the cell sizes in all three directions simultaneously to generate a medium mesh and successively a coarse mesh. Refinement ratios of $2^{1/2}$ (approximately 1.4) and 1.1 were also used on the fine mesh in an attempt to reduce cell sizes further; however, the mesh blocks was found impractical due to insufficient computer memory. As such, convergence of numerical results of some parameters of interest was not achieved in the grid sensitivity analysis. Table 1 shows the total active cell count and time required to complete simulations using the three mesh blocks and a 4-processor computer.

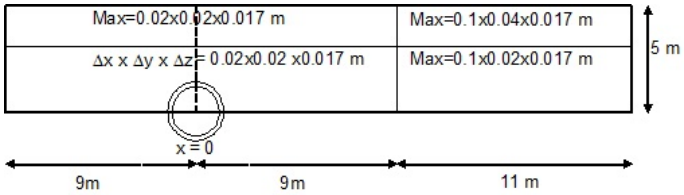

Figure 9. FINE MESH BLOCK (MODEL SCALE 1:40)

Table 1. MESH BLOCKS USED IN GRID SENSITIVITY ANALYSIS AND TIME TO COMPLETE SIMULATIONS

Mesh block	# of cells (million)	Time (days)	
		5 m, 6.9 sec wave	5 m, 8.4 sec wave
Fine	14.64	4.15	3.33
Medium	5.64	1.26	1.56
Coarse	2.01	0.31	0.41

Figure 10 shows example results from the grid sensitivity analysis. The predicted free surface elevations at most locations became very close to experimental data when the fine mesh was used. This showed the effectiveness of the mesh refinement scheme in reflecting sensitivity of free surface elevations to grid sizes and that the fine mesh was required to provide accurate green water predictions.

For the forces and bending moments, predicted x-forces in both cases matched the measured data well in all three mesh blocks. The z-forces calculated using the fine mesh were closest to the measured data except for the maximum z-force of the 8.4 sec wave. In addition, the z-force predictions were found most sensitive to resolution of the mesh block. Calculated y-moments did not match the measured values very well. However, the values obtained from all of the three mesh blocks were almost the same.

Calculated results from the fine mesh were expected to be more accurate as the mesh provided the most accurate representation of the GBS structure surface, which in turn affected the force and moment calculations. And thus, the fine mesh was selected and used to perform the CFD code validation for the LNG Terminal study.

Code Validation

In order to validate the CFD code using the physical model test results, simulations were conducted on model scale (1:40) and on only half of the structure by applying a symmetry plane at y = 0 along the wave propagation plane. In full scale, a numerical wave tank of 1160 meters length, 200 meters half-width, and 48 meters depth was created. Figure 11 shows the mesh block used.

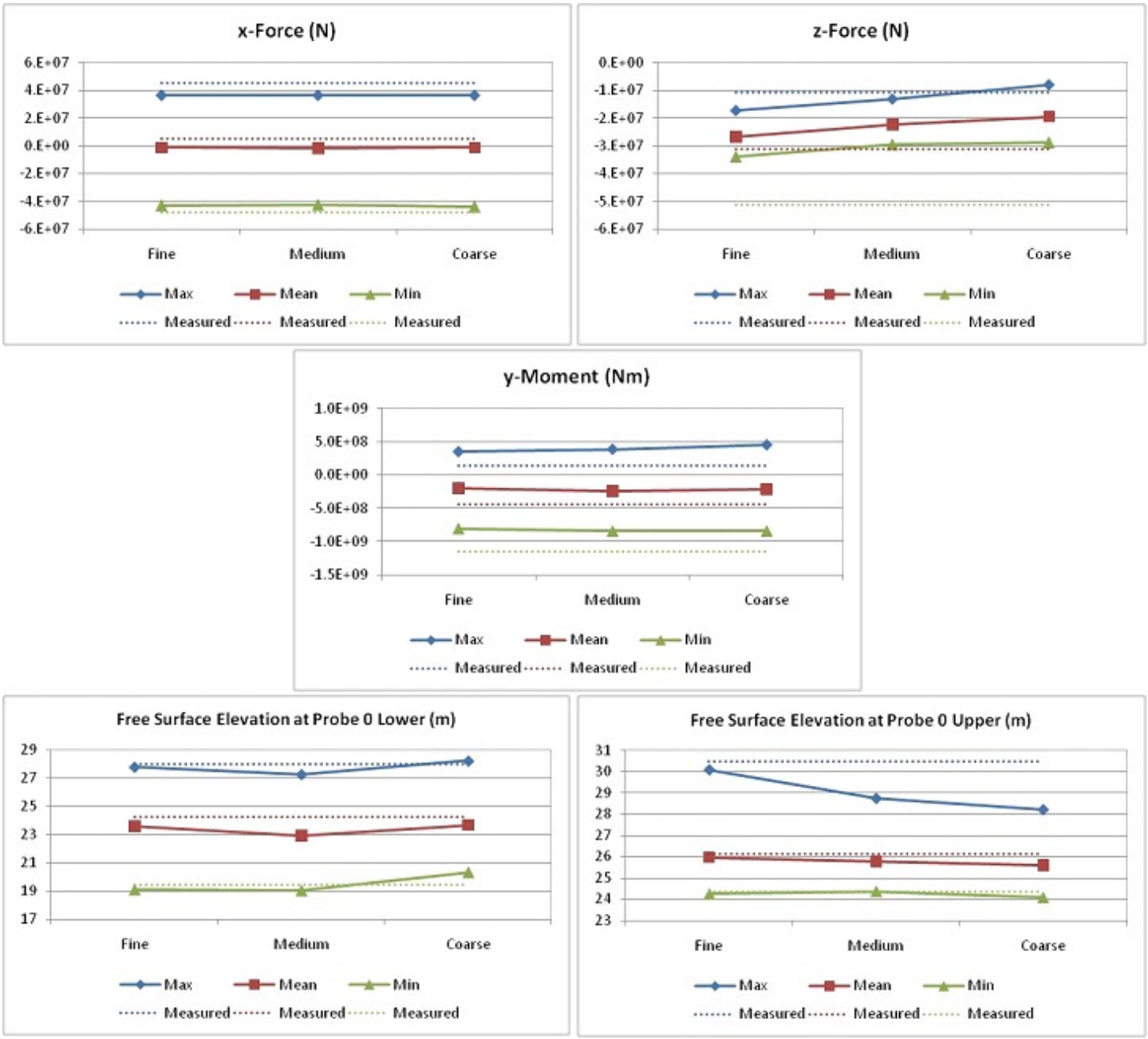

Figure 10. EXAMPLE RESULTS FROM 3 DIFFERENT MESH BLOCK RESOLUTIONS FOR 5.5 M 8.4 SEC WAVE

The tank was discretized using the fine mesh block as presented in the previous section (Figure 9). In full scale, the minimum cell width in the *x* and *y* directions (*dx* and *dy*) were 0.8 m close to the structure and the maximum of 4 and 1.6 m, respectively close to the walls. The depth of the tank was uniformly discretized using *dz*=0.68 m. Wave heights were first calibrated at the centre of the structure by running simulations without the structure. Once the desired wave heights were matched, the structure was added into the wave tank. For the waves simulated, approximately 30% and 9% of wave height increase were required for the 6.9 sec and 8.4 sec waves, respectively. The wave maker was approximately 4.5 diameters of the GBS away from the centre of the GBS. The origin of the coordinate was located at the centre of the GBS (x=0, y=0, z=0). The wave traveled in the +x direction with Wave and Outflow Boundary conditions applied at the –x and +x boundaries, respectively. Wall Boundary condition was applied at the bottom of the tank (z=0) and Symmetry Boundary conditions were used for side walls and the top of the tank (-y, y = 0, and +z boundaries). A porous wall was also used at the outflow boundary in order to maintain consistent fluid volume in the computational domain. However, the data analyzed were gathered from the time before the first wave reached the outflow boundary. Figure 12 shows a 3D snapshot of the wave pattern around the structure as well as green water coming on the base of the GBS. Figure 13 shows velocity vectors and wave run-up on the GBS at various points in time. Green water coming on the base of the structure can be obviously seen in the figures.

Figure 14 shows time history results of forces and bending moments acting on the structure. It can be seen that forces in the x-direction matched the experimental data very well. For forces in the z-direction and bending moments about the y-axis, the CFD analysis gave smoother, more uniform results for the case of wave with lower frequency. The code tended to overpredict bending moments espeically in the high frequency case. The z-forces were found to be underpredicted. However, the measured results may be less reliable in this regard as the physical model structure did not sit on the bottom of the wave tank but on the base of dynamometers leading to a small gap between the tank floor and the bottom of the structure. The reported z-force measurements were, however, corrected for the hydrodynamic pressure under the structure. The discrepancy of the z-force may also be influenced partly by inadequate vertical mesh refinement as well as the effects from the tank bottom in these shallow water cases. Figure 15 shows average maximum, mean, and average minumum values for x-forces, z-forces, and y-moments, respectively. Also shown in the figures are one standard deviation bands of each value.

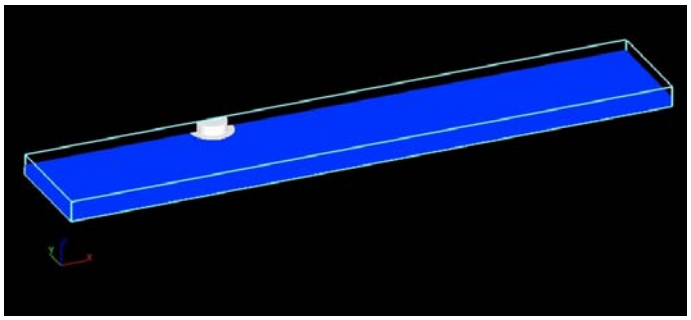

Figure 11. MESH BLOCK USED LNG TERMINAL SIMULATION

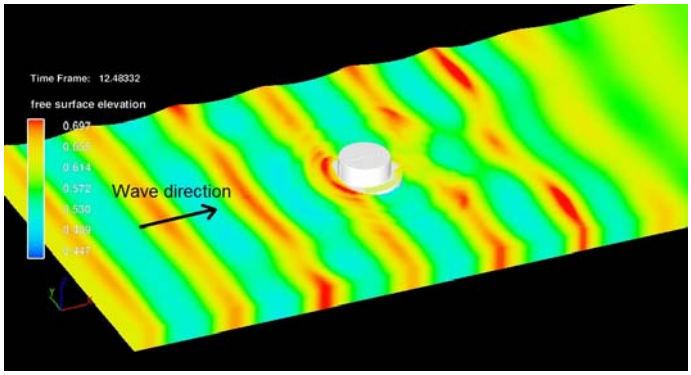

Figure 12. 3D IMAGE SHOWING WAVE PATTERN AROUND THE PROPOSED GBS FOR THE 5 M 8.4 SEC WAVE (MODEL SCALE)

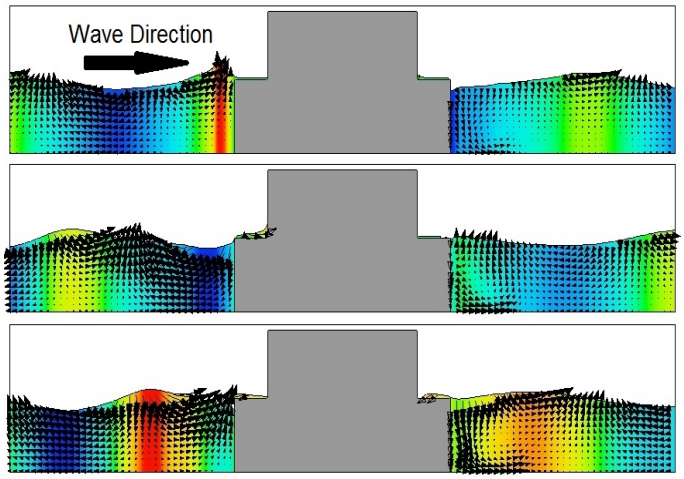

Figure 13. 2D IMAGE OF MODEL-SCALE SIMULATION OF THE 5 M 6.9 SEC WAVE AT SELECTED TIME; 17.60 SEC (TOP), 18.04 SEC (MIDDLE), AND 18.47 SEC (BOTTOM)

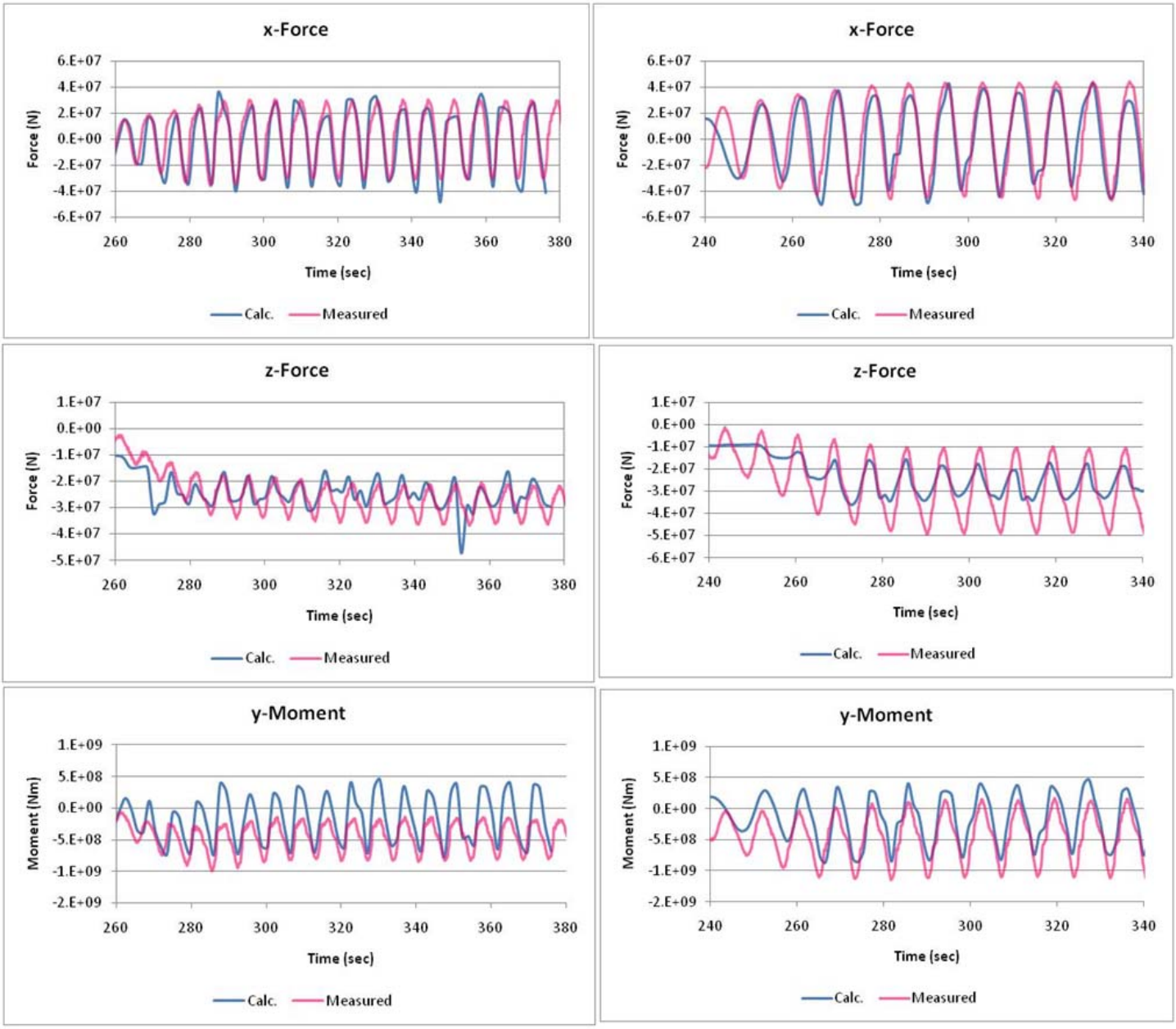

Figure 14. TIME HISTORY RESULTS OF FORCE AND BENDING MOMENT FOR 5.5 M 6.9 SEC WAVE (LEFT) AND 5.5 M 8.4 SEC WAVE (RIGHT)

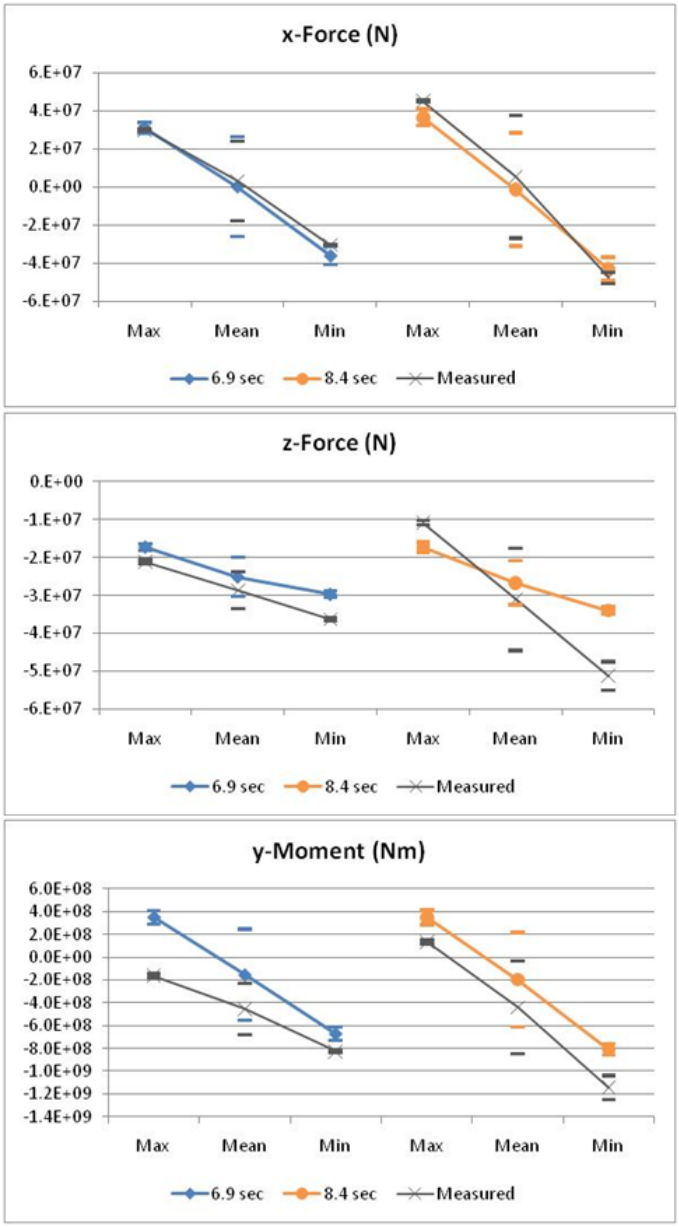

Figure 15. COMPARISONS OF FORCE AND BENDING MOMENT RESULTS FOR 5.5 M 6.9 SEC WAVE (LEFT) AND 5.5 M 8.4 SEC WAVE (RIGHT)

Figures 16 compares average wave heights. Figure 17 shows time history results of free surface elevations at probe locations around the GBS. The results from the experments are also plotted on the corresponding axes. It can be seen from the time history results that the predicted free surface elevations, particularly in terms of magnitude, are in good agreement with the measured values at all wave probe locations. Some non-linearities can also be seen. For upper wave probes, the minimum surface elevations predicted in the simlation were cut off at 24 meters which was the height of the structure base on which the probes were installed. Lower probe results show regular wave patterns with non-linearities. In addition, the model test results from the 170 Upper probe did not show much variation of surface elevation. This might be caused by the sensitivity of the probe used in the experiment. However, the mean values obtained from numerical analysis and physical tests are very close.

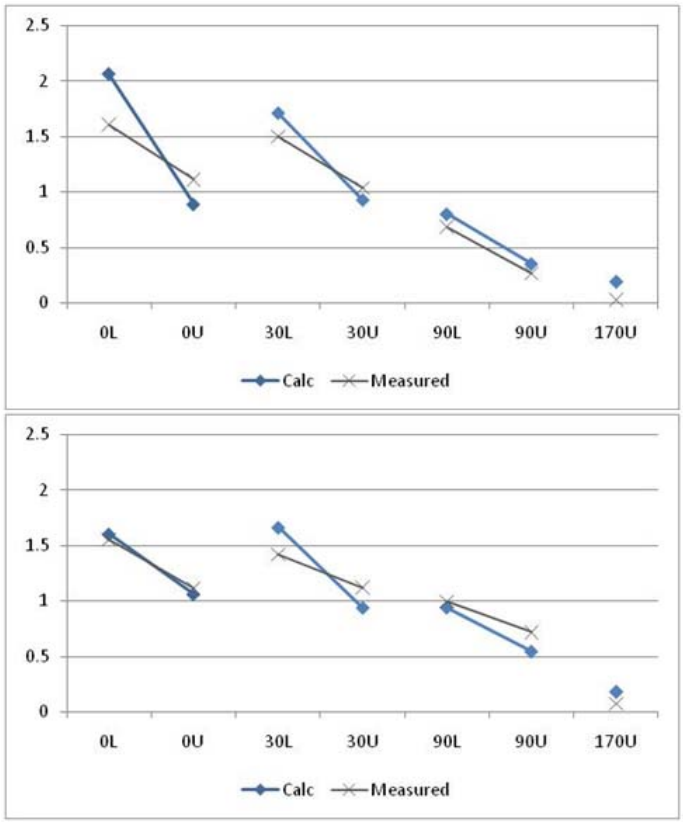

Figure 16. NORMALIZED AVERAGE HEIGHTS FOR 5.5 M 6.9 SEC WAVE (TOP) AND 5.5 M 8.4 SEC WAVE (BOTTOM)

CONCLUSION

This paper presented a comparison of the results of experiments on two types of offshore structure with the simulations using a Volume of Fluid- based CFD code. The focus of the simulations was the effects of waves on surface piercing structures. This study also considered forces and bending moments on GBS structures which are crucial parameters in the design of offshore structures. It was found from the study that the results generated by the code were in good agreement with observed non-linearities in the wave pattern close to the structure in each case, and that the method also gave good predictions of the measured forces and bending moments acting on the GBS. Grid sensitivity analysis was also conducted for the LNG Terminal case in order to find the optimal mesh resolution. Forces in the vertical direction were found most sensitive to mesh block resolution.

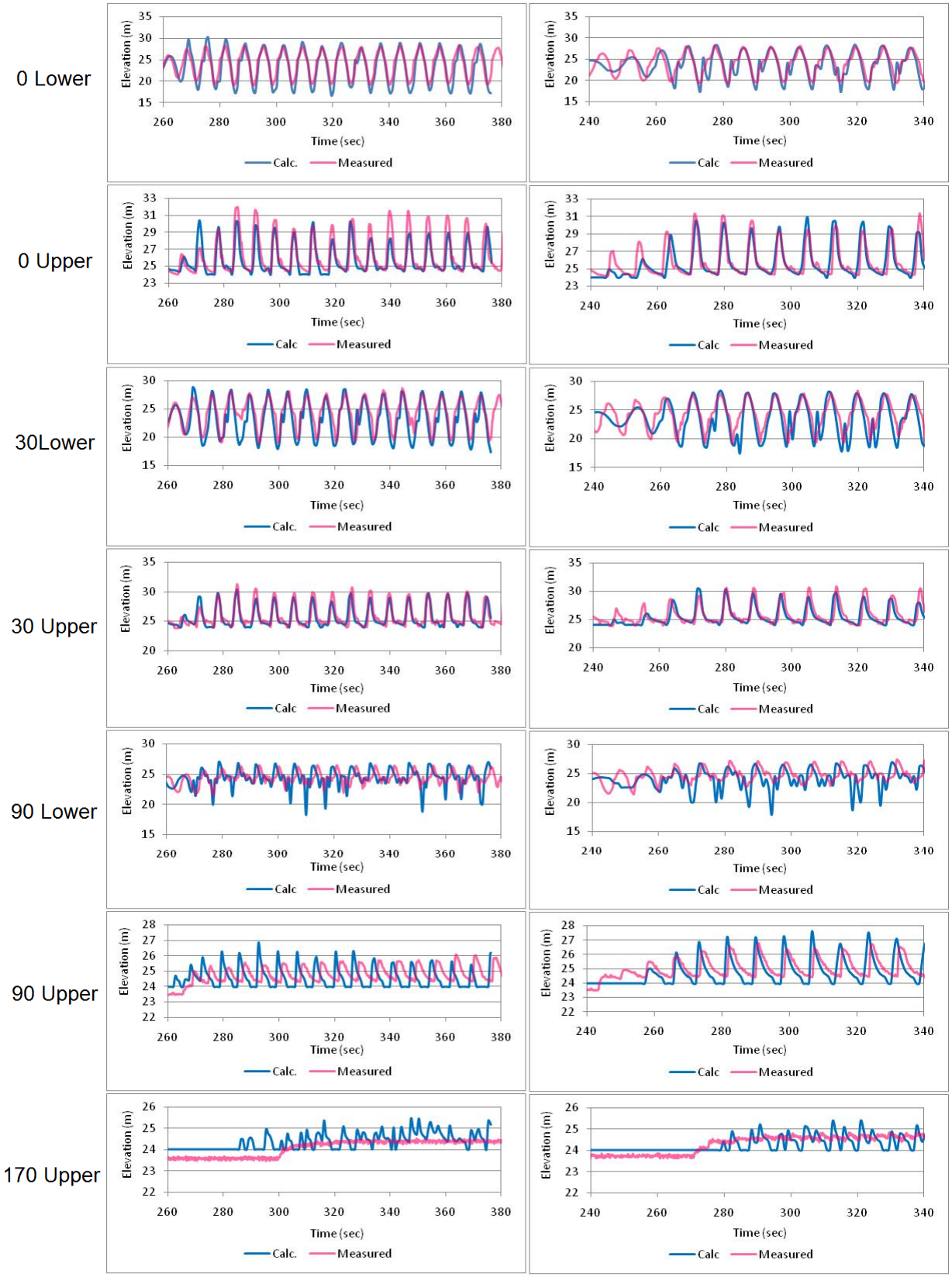

Figure 17. COMPARISONS OF CALCULATED AND EXPERIMENTAL TIME HISTORY RESULTS OF FREE SURFACE ELEVATIONS FOR 5.5 M 6.9 SEC WAVE (LEFT) AND 5.5 M 8.4 SEC WAVE (RIGHT)

ACKNOWLEDGMENTS

This work was carried out at Oceanic as part of a project which was supported by the Atlantic Innovation Fund administered by Atlantic Canada Opportunities Agency with additional financial support from Husky Energy Canada. The support from these two organizations is gratefully acknowledged.

REFERENCES

[1] Bass, D. W., Molyneux, W. D., McTaggart, K., 2004. Simulating Wave Action in the Well Deck of Landing Platform Dock Ships using Computational Fluid Dynamics, Conference paper presented at the *Warship 2004, London, England.* NPArC# 8895748

[2] Flow Science Inc., 2009. *Flow-3D User Manual* Version 9.4

[3] Trulsen, K. and Teigen, P., 2002. Wave Scattering Around a Vertical Cylinder: Fully Nonlinear Potential Flow Calculations Compared with Low Order Perturbation Results and Experiment. In *Proceedings of OMAE'02, 21st International Conference on Offshore Mechanics and Arctic Engineering, June 23 – 28, 2002, Oslo, Norway*.

[4] ITTC., 2008. *Uncertainty Analysis in CFD Verification and Validation Methodology and Procedures*. ITTC– Recommended Procedures and Guidelines, 7.5-03-01-01.